Pre-organization of diarylideneacetonyl crownophanes in single crystals to photochemical transformations

I. G. Ovchinnikova,[a]★ *D. K. Nikulov,*[b] *E. V. Bartashevich,*[b] *E. G. Matochkina,*[a] *M. I. Kodess,*[a] *P. A. Slepukhin,*[a] *A. V. Druzhinin,*[c] *O. V. Fedorova,*[a] *G. L. Rusinov,*[a] *and V. N. Charushin*[a]

[a]*I. Ya. Postovsky Institute of Organic Synthesis, Ural Branch of the Russian Academy of Sciences, 22/20 ul. S. Kovalevskoi, 620990 Ekaterinburg, Russian Federation. Fax: +7 (343) 369 3058. E-mail: iov@ios.uran.ru*

[b]*Southern-Ural State University, 76 prosp. Lenina, 454080 Chelyabinsk, Russian Federation. E-mail: kbartash@yandex.ru*

[c]*Institute of Metal Physics, Ural Branch of the Russian Academy of Sciences, 18 ul. S. Kovalevskoi, 620041 Ekaterinburg, Russian Federation. E-mail: druzhimin@imp.uran.ru*

Specific features of crystal packings and pre-organization of diarylideneacetonyl crownophane molecules to solid-phase photochemical transformations were studied on the basis of X-ray diffraction data using methods of simulation of molecular crystal packings. The tendency of the most part of the synthesized macrocyclic *E*,*E*-isomers to the formation of homochiral crystals ($P2_12_12_1$) was revealed, while (23*E*,26*E*)-11,12,14,15-tetrahydro-8*H*-dinaphtho-[2,1-*k*:1´,2´-*r*][1,4,7,10]tetraoxacyclononadecine-23,26-dien-25(9*H*)-one is prone to polymorphism. A phenomenon of solid-phase stereospecific photochemical dimerization of molecules according to the *syn*-head-to-tail type without crystal destruction (single crystal—single crystal transformation) was found for one of the modifications of this crownophane.

Key words: crownophanes, [2+2] photocycloaddition, topochemical control, α-truxillic structure, photochemical transformation single crystal—single crystal.

Engineering of highly organized photocontrolled molecular structures (in concentrated solutions, films, and solid phase, including single crystals) is one of priority directions of supramolecular chemistry.[1,2] Target synthesis of similar supramolecular architectures is mainly related to the solution of such problems as the creation of conditions for stereospecific photochemical transformations of molecules in single crystals with the simultaneous retention of the crystals themselves due to photolysis (transformations of the single crystal—single crystal type).[3] Various derivatives of cinnamic acid and (aza)stilbenes capable of reacting in photoinduced [2+2] cycloaddition (PCA) found wide use as building blocks.[4—11] It was shown in a series of works that stereospecificity of PCA processes depends directly on the ability of alkenes in crystals to form sandwich dimers (α- or β-forms) with ethylene bonds optimally approached to each other (3.3—4.2 Å).[2—6]

Presently, two main approaches to form dimers in crystals can be distinguished. The first of them is related to the use of templates (metal ions as salts and complexes or polar organic molecules), which can direct self-assembly of photochromic molecules in sandwiches during crystallization through nonvalent interactions and also can form loose zones for the retention of the crystal lattice during photolysis.[3,12—30] The second approach is based in imparting analogous properties to olefin molecules themselves by the introductions of certain functional groups. The template properties[2,3,31,32] can be controlled by the introduction of halogen atoms and carboxyl, hydroxyl, amino, and other groups, and the capability of forming loose zones between the molecular dimers[33—39] can be controlled by the introduction of bulky substituents, for instance, branched aliphatic residues or polyether fragments when using macroheterocycles as building blocks. Crown-containing (aza)stilbenes were used[33—39] to construct photosensitive supramolecular ensembles. An exclusively important role of the conformationally mobile polyether fragment was demonstrated for the formation of intermolecular sandwich dimers and for controlling molecular geometry during PCA in crystals without their destruction. In turn, we synthesized acyclic analogs of crown ethers, chalcone podands, and showed their tendency to form intermolecular sandwiches in crystals and the possibility of some of them to undergo PCA reactions in the solid phase.[40,41]

Continuing our works on the study of the photochromic properties of macrocycles and their open-chain analogs,

Published in Russian in *Izvestiya Akademii Nauk. Seriya Khimicheskaya,* No. 5, pp. 805—820, May, 2011.

we synthesized diarylideneacetonyl crownophanes in which the dienone and oligooxyethylene fragments in combined in one macroheterocycle. The main packing motifs and parameters of pre-organization of the crownophanes to photochemical transformations, including PCA, in single crystals were revealed by X-ray diffraction analysis.

Results and Discussion

Molecular and crystal structures of crownophanes. The condensation of formyl podands **1—4** with acetone in the presence of potassium hydroxide gave crownophanes **5—8** predominantly as *E*,*E*-isomers in 25—42% yields (Scheme 1). The content of the *E*,*Z*-adducts in the reaction mixtures of compounds **5—8** varied within 5—12% according to the data of ^{1}H NMR spectroscopy. In particular, the formation of *E*,*Z*-isomer **7** is confirmed by the presence in the spectra of four doublets of the α,β-protons of the CH=CH groups at δ 6.58, 7.84 and 6.84, 7.30 with spins-spin coupling constants (SSCC) of 16.5 and 12.5 Hz, respectively.

The molecules in crystals of *E*,*E*-crownophanes **5—8** (Figs 1—8), which can formally be assigned to compounds with symmetry C_2, has symmetry C_1 due to differences in the conformational and geometric parameters of the oligooxyethylene and chromophoric fragments. The pentadienone fragment in the molecules is almost planar. The deviation of the carbon atom of the C=O group from the root-mean-square plane passed through the carbon atoms of the C=C fragments varies within 0.07—0.28 Å. The bond length distribution in the dienone frag-

Scheme 1

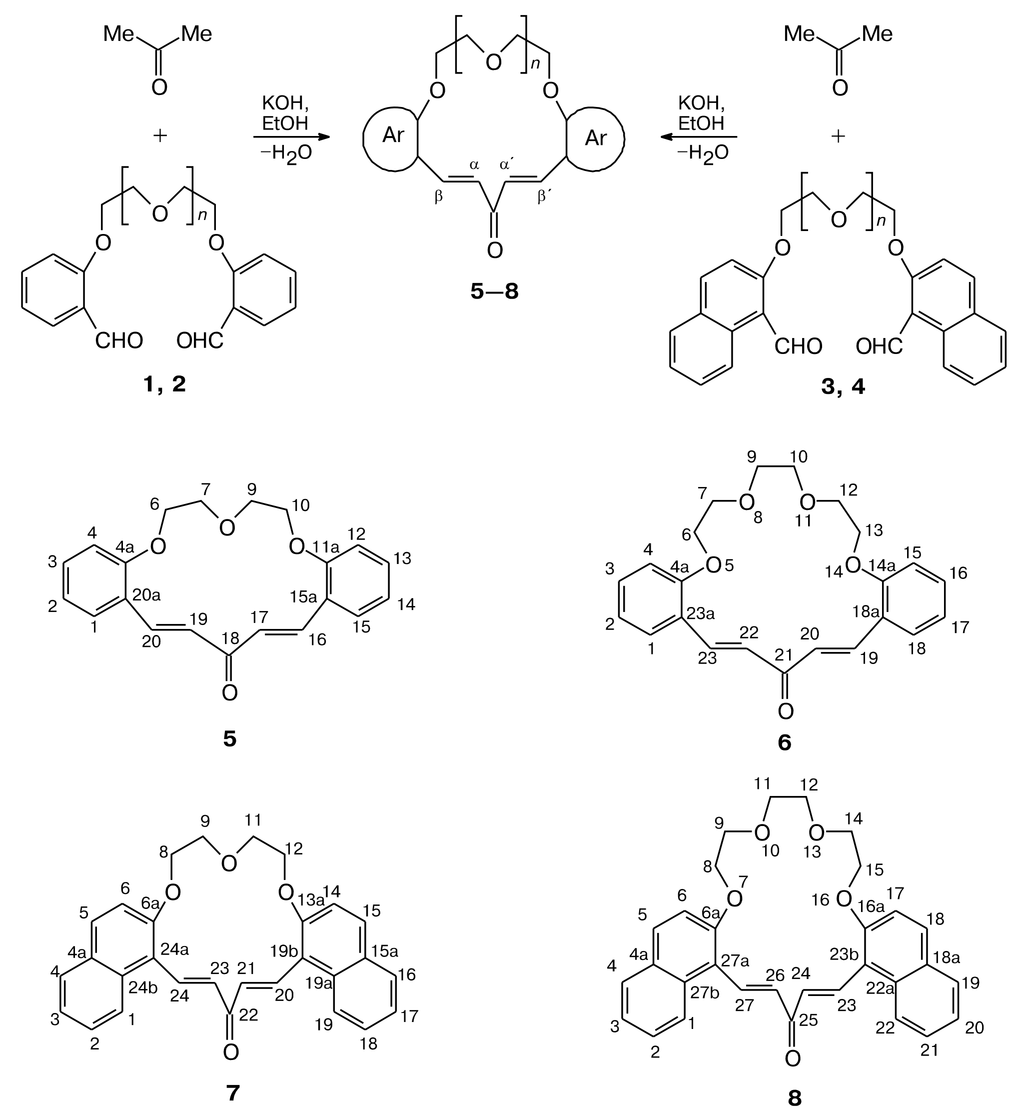

1, **5**: *n* = 1, Ar = Ph; **2**, **6**: *n* = 2, Ar = Ph; **3**, **7**: *n* = 1, Ar is naphthyl; **4**, **8**: *n* = 2, Ar is naphthyl.

ment of crownophane molecules is analogous to that observed earlier[40,41] in the propenone fragments of the chalcone podands. The bond lengths of the fragment C(1)—C(21)=C(20)—C(19)—C(18)=C(17)—C(16) in compound **5** are 1.456(3), 1.327(3), 1.467(3), 1.465(3), 1.323(3), and 1.444(3) Å; those of C(12)—C(11)=C(10)—C(9)—C(8)=C(7)—C(6) in compound **6** are 1.446(3), 1.328(3), 1.470(3), 1.471(3), 1.328(3), and 1.447(3) Å; C(10)—C(11)=C(12)—C(13)—C(14)=C(15)—C(16) in compound **7** are 1.4625(19), 1.331(2), 1.466(2), 1.472(2), 1.309(2), and 1.4552(19) Å; C(10)—C(11)=C(12)—C(13)—C(14)=C(15)—C(16) in compound **8a** are 1.454(2), 1.323(2), 1.465(2), 1.469(2), 1.319(2), and 1.459(2) Å; and those of C(10)—C(11)=C(12)—C(13)—C(14)=C(15)—C(16) in compound **8b** are 1.466(4), 1.330(4), 1.461(4), 1.460(4), 1.342(4), and 1.453(4) Å. However, unlike chalcone groups, the pentadienone fragment of crownophane molecules demonstrates greater conformational and configurational diversity. Molecules of *E*,*E*-isomers **5** and **7** ($n = 1$) in crystals prefer *trans-S-cis-S-trans-trans*-isomerism (*S-cis-* or *S-trans*-conformation of the C=C—C=O fragment caused by hindered rotation about the simple sp^2—sp^2 bond (carbon—carbon) of the polyene fragment (see Figs 1 and 5). With the elongation of the polyether chain on going to compounds **6** and **8** ($n = 2$), the pentadienone fragment gains the *trans-S-cis-S-cis-trans*-configuration (see Figs 3, 7, and 8).

According to the data of ^1H and ^{13}C NMR spectroscopy, in solutions compounds **5—8** exist in the "symmetrical" form. The *trans*-configuration of the double bonds is confirmed by the values of vicinal SSCC $J_{\alpha,\beta}$ ($J_{\alpha',\beta'}$) ≈ 16 Hz (Table 1). However, the results of 2D NOESY experiments indicate differences in conformations of the pentadienone fragments of molecules **5—8**. The cross-peaks between the *ortho*-protons of the phenyl substituent or the protons at C(1) and C(22) of the naphthyl substituent and the olefinic proton H_β appears in the spectra of compounds **6** and **8** ($n = 2$), which is quite consistent with the *trans-S-cis-S-cis-trans*-conformation similar to the corresponding fragment of the molecules in crystals. In the 2D NOESY

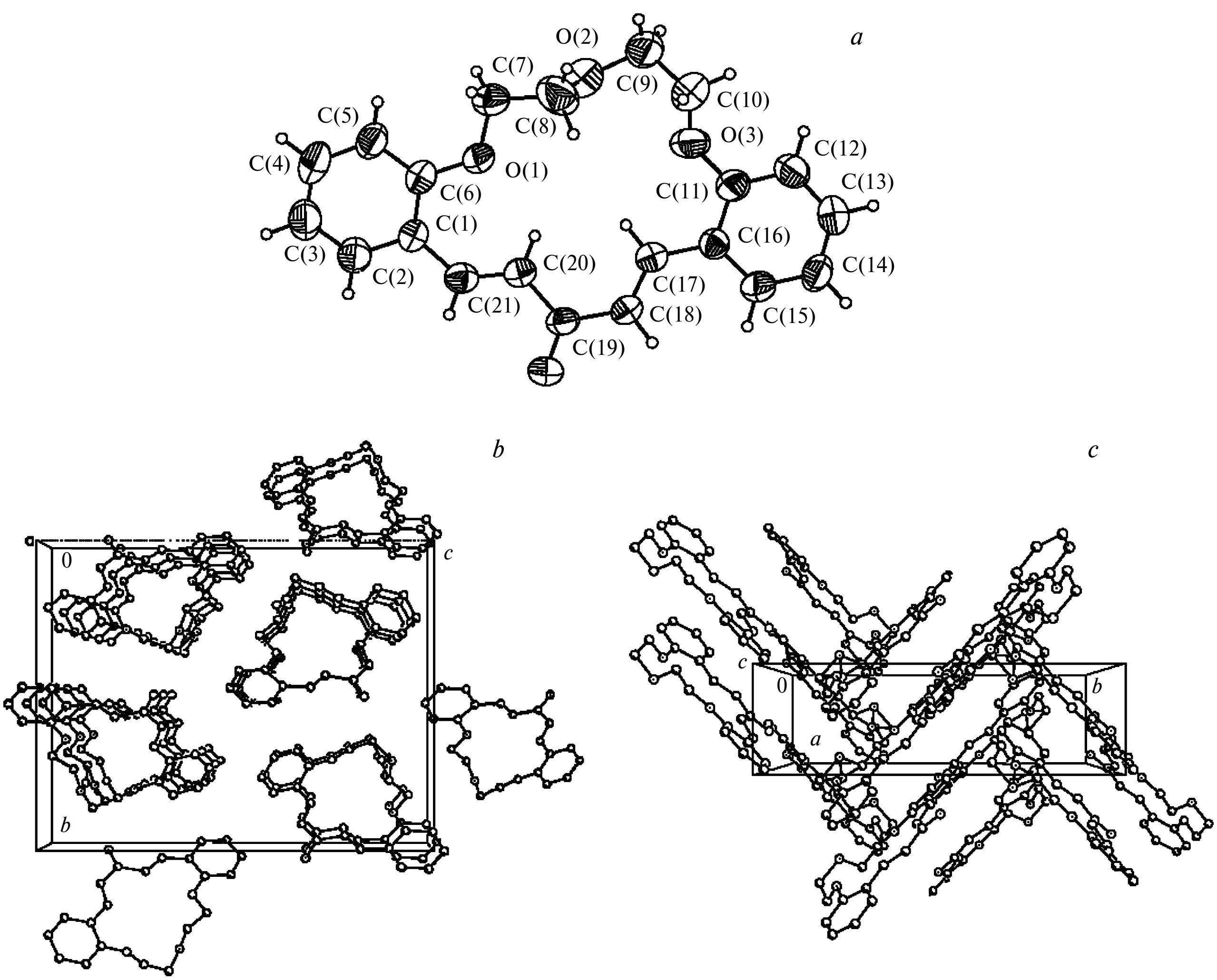

Fig. 1. Molecular geometry (*a*) and molecular packing (translation along the axes *a* (*b*) and *c* (*c*)) for crownophane **5**.

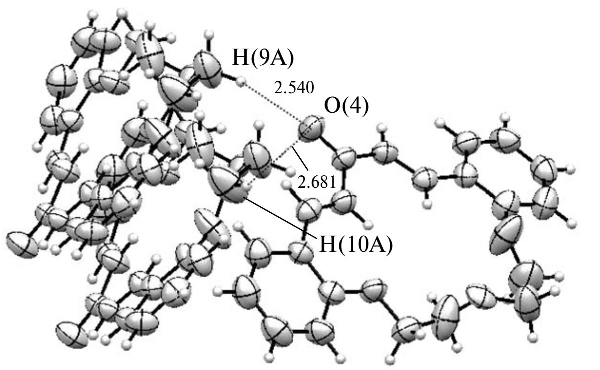

Fig. 2. Selected shortened intermolecular contacts (Å) in packing of crownophane **5**.

spectra of compounds **5** and **7** (n = 1), the *ortho*-protons of the phenyl substituent and the protons at C(1) and C(19) of the naphthyl substituent give cross-peaks with H_β and H_α of approximately equal intensity, indicating that the *trans*-*S*-*trans*-*S*-*trans*-*trans*-conformation is present in solution and the conjugation of the aromatic cycle and double bond is partially distorted. A comparison of the X-ray diffraction and NMR spectroscopic data for crownophanes **5** and **7** indicates the conformational transformation of one rotamer into another upon dissolution.

Intermolecular bringing together of the photosensitive CH=CH bonds of the pentadienone fragment in packings is affected not only by the spatial architecture of the crownophane molecules themselves in crystals and geometrical specific features of the functional groups but also by their adjacent environment[2,42] (topotactic control of crystal lattice).

According to the X-ray diffraction data, *E*,*E*-isomers **5**—**7** crystallize in the non-centrosymmetric space group $P2_12_12_1$. Molecules of crownophanes **5** and **6** with phenyl substituents form a ladder packing lying along one of the axes with a displacement of the head-to-head type (see Figs 1 and 3). As can be seen from the figures, the molecules are almost planar, the benzene rings

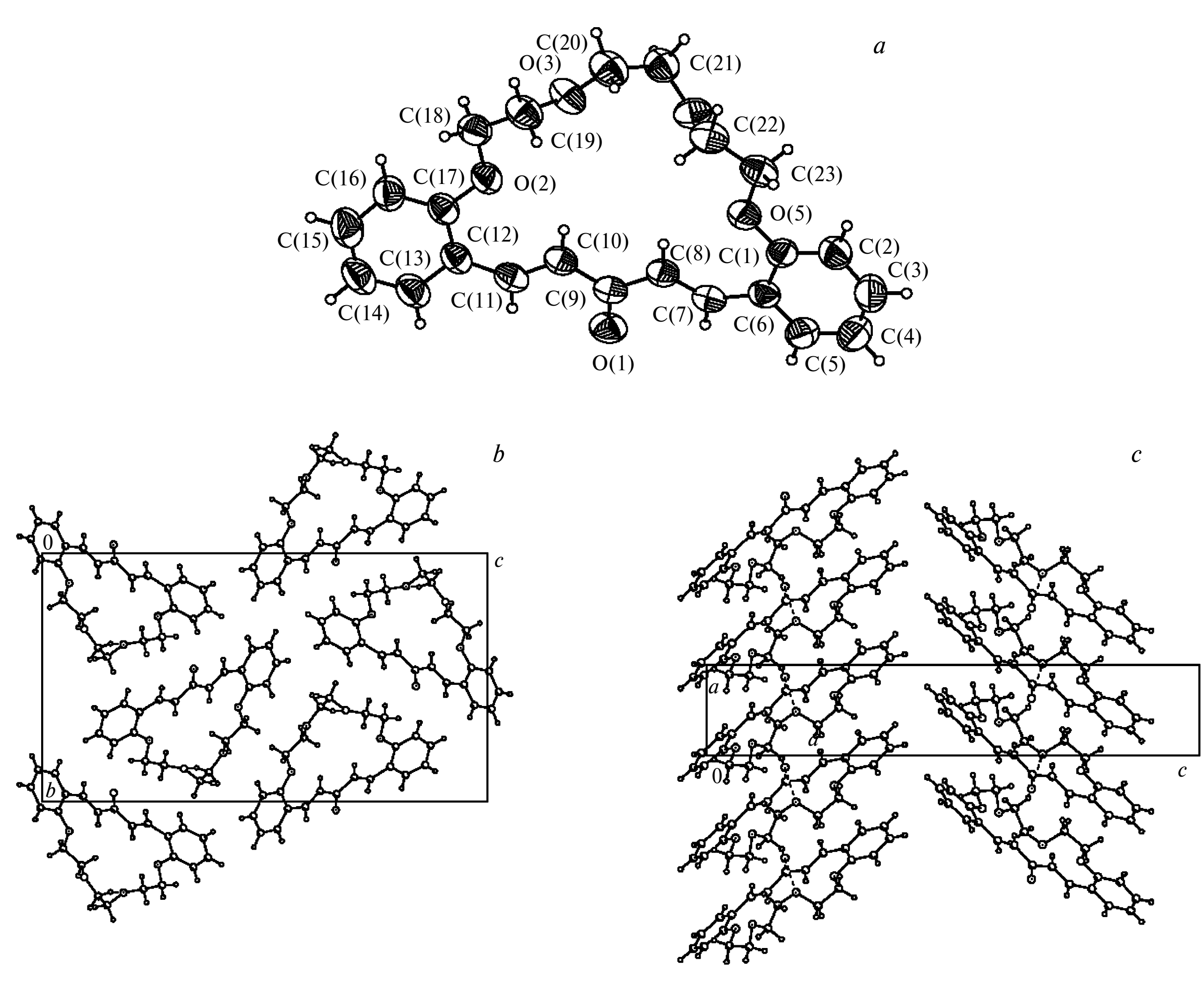

Fig. 3. Molecular geometry (*a*) and molecular packing (translation along the axis *a* (*b*)) for crownophane **6**.

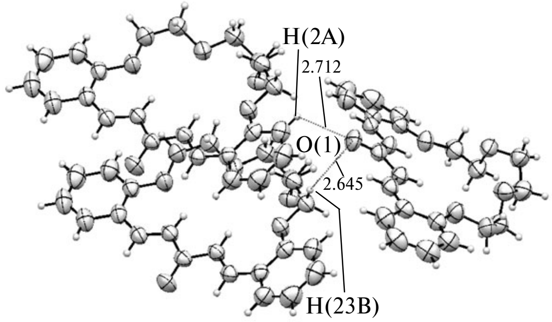

Fig. 4. Selected shortened intermolecular contacts (Å) in packing of crownophane **6**.

Table 1. Chemical shifts (δ) and SSCC of the —CH=CH— group ($J_{\alpha,\beta}$) of the pentadienone fragment in crownophanes **5**—**8**

Compound	δ					$^3J_{\alpha,\beta}$/Hz
	H_α	H_β	$\Delta_{\alpha,\beta}$	C_α	C_β	
5	7.54	7.92	−0.38	126.03	138.72	16.4
6	7.50	7.64	−0.14	128.44	139.70	15.9
7	7.70	8.48	−0.78	129.35	135.62	16.4
8	7.79	8.45	−0.66	131.20	133.87	15.6

C(1)...C(6)/C(11)...C(16) are turned from the plane of the pentadienone fragment C(21)C(20)C(18)C(17) for compound **5** and C(1)...C(6)/C(12)...C(17) from the plane C(11)C(10)C(8)C(7) for compound **6** by the angles 11.2/7.8 and 10.9/10.9°, respectively. The packings exhibit predominantly shortened intermolecular contacts at the level of van der Waals radii of interaction between the oxygen atoms of the C=O group and hydrogen of the oxyethylene fragment. The distances O(4)...H(4a) [$-1+x, y, z$] and O(4)...H(10b) [$1/2+x, 1/2-y, 1-z$] are 2.54 and 2.68 Å, respectively, for crownophane **5**, and O(1)...H(2a) [$-x, -1/2+y, 1/2-z$] and O(1)...H(23b) [$1-x, -1/2+y, 1/2-z$] for crownophane **6** are 2.71 and 2.64 Å (see Fig. 4). There are no π-staking overlapping zones between the aromatic fragments due to the displacement of adjacent molecules in piles, and the intermolecular distances between the C=C bonds of the enone fragments are 4.8—4.9 Å.

On the contrary, on going to naphthyl-containing crownophane **7**, the aromatic substituents shift from the root-mean-square plane of the pentadienone fragment of the molecule (see Fig. 5). The naphthyl rings C(1)...C(10)/C(16)...C(25) are unfolded from the plane of the polyene fragment C(11)C(12)C(14)C(15) for compound **7** by the angles 44.7/13.8°. In this case, the crystal lattice is formed by parquet-ladder packing in which the aromatic systems of each molecule from adjacent piles are brought together to 3.79—3.41 Å (the distance between the centroids C(4)...C(9) and C(4a)...C(9a) is 3.79 Å) additionally supported by the T-shaped intermolecular shortened contacts C—H...π(Ar) (see Figs 5 and 6). The distances C(21)...H(3a) [$1-x, +1/2+y, 1/2-z$], C(22)...H(3a) [$1-x, +1/2+y, 1/2-z$], and C(25)...H(23a) [$-1/2+x, 1/2-y, 1-z$] are 2.81, 2.84, and 2.82 Å, respectively. Similarly to compounds **5** and **6**, the molecules are packed in piles by the head-to-head type. However, the elongation of the shortened intermolecular contacts results in the lateral shift of the molecules to the interpile zones and undesirable elongation of the distance between the C=C bonds of the enone fragments of adjacent molecules in piles to 6.9 Å.

Polymorphism[2] was found for compound **8** with the longer oligooxyethylene fragment (see Figs 7 and 8). In the case of modification **8a** that crystallizes from a pyridine solution in the space group *C*2/c, crownophane molecules exhibits a considerable shift of aromatic substituents from the root-mean-square plane of the pentadienone fragment similar to that in compound **7**, and the naphthyl rings C(1)...C(10)/C(16)...C(25) are unfolded relative to the plane C(11)C(12)C(14)C(15) by 42.8/29°. In the case of modification **8b** that crystallizes from an acetonitrile solution in the space group $P2_1/c$, and the molecules have an almost planar geometry with the rings C(1)...C(10)/C(16)...C(25) unfolded from the plane C(11)C(12)C(14)C(15) by the angles 5.2/7.8°. Nevertheless, regardless of polymorphic modification **8a** or **8b**, the molecules in crystals are packed as centrosymmetric dimers by the head-to-tail type, forming parquet-

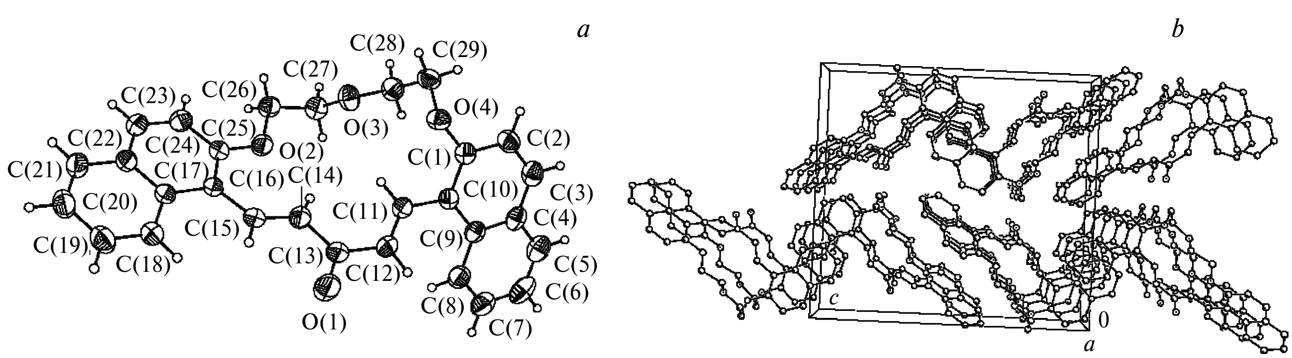

Fig. 5. Molecular geometry (*a*) and molecular packing (translation along the axis *a* (*b*)) for crownophane **7**.

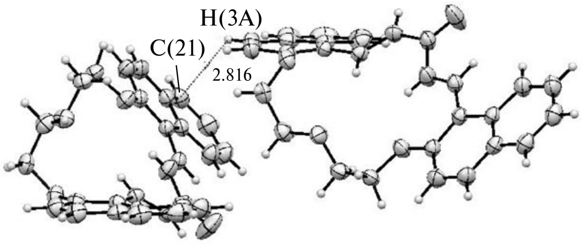

Fig. 6. Selected shortened intermolecular contacts (Å) in packing of crownophane **7**.

ladder packing. Such a supramolecular architecture of molecular lattice is additionally stabilized by the involvement of the both naphthyl substituents of each adjacent molecule into the π-stacking zones of interaction to form pseudo-oligomeric chains due to translation of dimers along one of the axes (see Figs 7—9). Crystalline modification **8a** contains only partial, formed along the "aromatic periphery" of molecules stacking overlapping zones separated by loose zones of bulky polyether chains, which prevent bringing together the C=C bonds of the pentadienone fragments of the molecules. On the contrary, in centrosymmetric dimers **8b** almost full sandwich overlapping zones involving the whole conjugated chromophoric fragment of the molecules are formed due to molecular geometry flattening (see Fig. 9). For this packing type, the distance between the C=C bonds of the enone fragments of the molecules reaches a value optimal for the PCA reaction to occur: 3.5 Å.

Structural specific features of crownophanes **5—8** in crystals related to the presence of diarylideneacetonyl and coordinatively mobile polyether fragments make it possible to classify them along with such compounds as

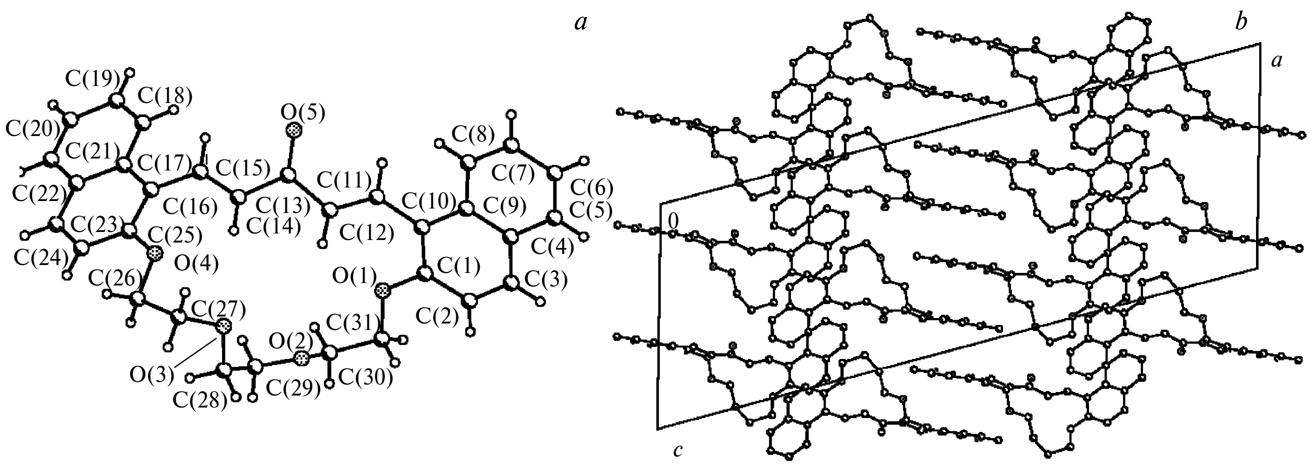

Fig. 7. Molecular geometry (*a*) and molecular packing (translation along the axis *b* (*b*)) for crownophane **8a**.

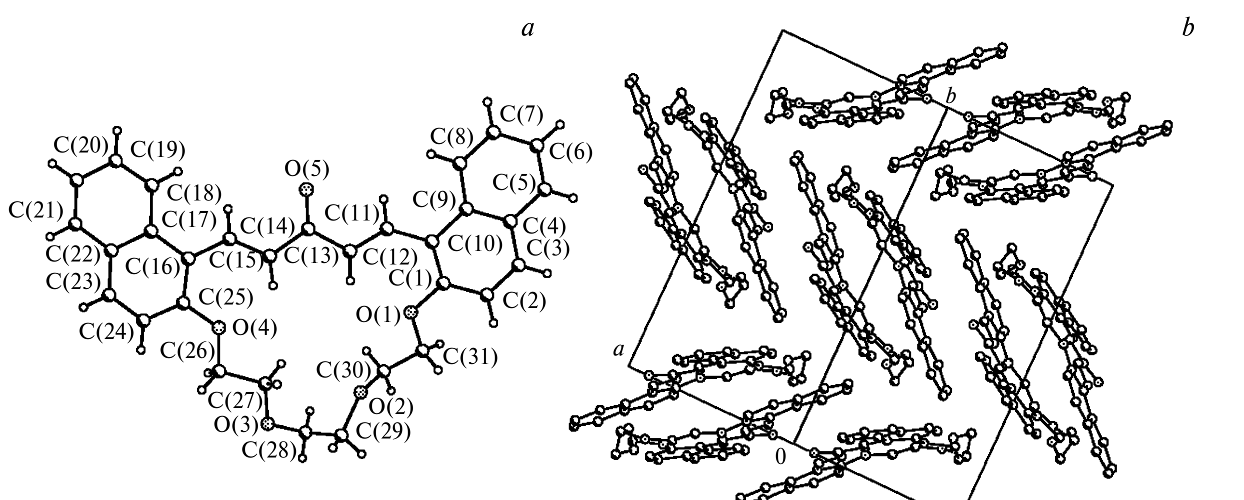

Fig. 8. Molecular geometry (*a*) and molecular packing (translation along the diagonal along the axes *a* and *c* (*b*)) for crownophane **8b**.

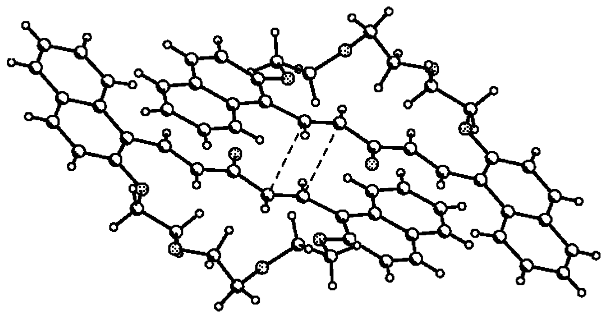

Fig. 9. Centrosymmetric dimer **8b**.

atropoisomers, helicates, alkylidenecycloalkanes, cyclophanes, and others, whose molecules can demonstrate, under certain conditions, axial and/or planar chirality (varieties of spirality).[43—45] In crownophanes asymmetry appears due to hindered conformational transitions in the crystal packing and is caused by the shift of the polyether chain with spiral geometry from the plane of the dienone fragment of the molecule. In particular, the oligooxyethylene fragment in molecules of crownophane **7** has the conformational sequence a-$g^{(-)}$-a-a-$g^{(+)}$-$g^{(+)}$ of units —O—CH_2—CH_2—O— (see Fig. 5).[46] The torsion angles C(25)O(2)C(26)C(27), O(2)C(26)C(27)O(3), C(26)C(27)O(3)C(28), C(27)O(3)C(28)C(29), O(3)C(28)C(29)O(4), and C(28)C(29)O(4)C(1) are 177.65, −69.43, −166.94, −178.33, 65.45, and 76.39°, respectively. The shift of the oligooxyethylene chain from the pentadienone fragment plane varies from 0.95 to 1.53 Å (distance from C(27) and O(4), respectively, to the plane C(11)C(12)C(14)C(15)). Similar spiral geometry of the oligooxyethylene segment is characteristic of molecules of chalcone podands (C_2 symmetry), *viz*., acyclic analogs of diarylideneacetonyl crownophanes, in crystals.[40,41] It is not excluded that in compounds **5—7** the ability to form crystals in the chiral space group of symmetry $P2_12_12_1$ is related, first of all, to conformational isomerism[2] of the polyether fragment of the molecules (Table 2).

Using methods of simulation of molecular crystal packings (see Experimental), we attempted to evaluate the probability of formation of homochiral and heterochiral crystals and the influence of structure-forming features of the model packings (conformational effects, replacement of phenyl and naphthyl fragments in molecules, *etc*.) on the approaching of internuclear distances of potentially possible reaction centers $C_{\alpha}...C_{\beta}$ and/or $C_{\alpha'}...C_{\beta'}$ of the molecules neighboring in crystal.

Simulation quality was evaluated by a comparison of packings of model structures and X-ray diffraction experimental data. It was found that the simulation results reproduce the geometric structure and crystalline motifs of four of five crystal structures considered. Each of such sets containing 60 generated packings contains structures that agree qualitatively with the X-ray diffraction data. The quality of packing reproduction was evaluated by the superimposition of crystal fragments of the generated structures of the structures established by X-ray diffraction, and the number of molecules, whose positions coincide, was finally determined. If the number of coincidences was 50%, we concluded that the packings resemble satisfactorily; if the number of coincidence exceeded 75%, we decided that the packing is well reproduced. Therefore, if the positions of all molecules coincided in the model and real crystals, the crystal packing was considered reproduced.

The best quality of packing reproduction is observed for compound **6**: the model structure with the energy minimum corresponds to that obtained experimentally (Table 3). For compound **5**, the structure reproducing the crystal packing was obtained in the group $P2_12_12_1$ with the minimum value of energy in this space group (−183.86 kJ mol^{-1}). For compound **8b**, the structure satisfactorily reproducing the packing was found in the space group $P\bar{1}$. For compound **8a**, the crystal lattice structure was well reproduced in the space group $P2_1/c$ with the minimum energy. Among the simulated packings, the most approaching of the reaction centers $C_{\alpha}...C_{\beta}$ is observed for compound **5** in the space group $C2/c$ in two structures close in energies (−163.08 and −163.86 kJ mol^{-1}). The distance corresponding to approaching of the reaction centers $D_{C_{\alpha}...C_{\beta}}$ is 3.252 and 3.258 Å, respectively. However, the values of energies of this crystal lattice are comparatively high compared to the minimum value for the compound in the group $P2_1/c$ (−185.05 kJ mol^{-1}). Thus, the structure packing in this group resulting in the favorable approaching of the reaction centers should be considered as thermodynamically less probable than the structures having a lower lattice energy (see Table 3).

The simulation results in the heterochiral space groups $C2/c$, $P2_1/c$, and *Pbca* show the possibility of formation of the very diverse motifs of packings for all considered structures of crownophanes **5—8**. Space group $P\bar{1}$ is characterized by the pile packing of π-systems with the predominant head-to-head packing type. In the generated homochiral space groups $P2_12_12_1$ and $P2_1$, the predominant motifs of analogous packing of pairs of brought together crownophanes are also piles in which the π-systems are arranged in parallel planes (Fig. 10). These sets include weak interpile hydrogen bonds C=O...H—C, probably, stabilizing the packing. When imposing conditions of choosing three packings with the lowest lattice energies for each space group, one can observe a hypothetical possibility of both heterochiral and homochiral packings for the compounds to take place(see Table 3, Fig. 10). It is essential that for compounds **5**, **6**, and **8a** the values of energies of homochiral packings mainly lie in the region of lowest values, while they occupy an intermediate position for crownophane **7**. These results agree with the experimental data: homochiral packings are observed for structures **5—7**. However, if the factor of approaching

Table 2. Parameters of crystals and X-ray diffraction experiments for compounds **5—9**

Parameter	**5**	**6**	**7**	**8a**	**8b**	**9**
Molecular formula	$C_{21}H_{20}O_4$	$C_{23}H_{24}O_5$	$C_{29}H_{24}O_4$	$C_{31}H_{28}O_5$	$C_{31}H_{28}O_5$	$C_{62}H_{56}O_0$
Molecular weight /g mol^{-1}	336.37	380.42	436.48	480.53	480.53	961.07
Crystal system	Orthorhombic	Orthorhombic	Orthorhombic	Monoclinic	Monoclinic	Monoclinic
Z	4	4	4	8	4	2
Space group	$P2_12_12_1$	$P2_12_12_1$	$P2_12_12_1$	$C2$/c	$P2_1$/c	$P2_1$/c
a/Å	4.9371(9)	4.8736(2)	6.9070(4)	39.218(4)	15.490(2)	15.309(3)
b/Å	16.396(2)	14.8649(6)	16.9982(9)	9.0837(8)	16.842(2)	16.601(3)
c/Å	20.902(4)	26.6993(13)	16.9982(9)	14.2518(14)	9.1939(12)	9.251(2)
α/deg	90	90	90	90	90	90
β/deg	90	90	90	105.957(9)	98.407(11)	98.242(18)
γ/deg	90	90	90	90	90	90
V/Å^3	1692.0(5)	1934.25(15)	2171.2(3)	4881.6(8)	2372.8(5)	2326.9(9)
d_{calc}/g cm^{-3}	1.320	1.306	1.335	1.308	1.345	1.372
F(000)	712	808	920	2032	1016	1016
μ(Mo-Kα)/mm^{-1}	0.091	0.091	0.088	0.088	0.090	0.092
Crystal size/mm	0.50×0.18×0.06	0.41×0.22×0.08	0.46×0.39×0.22	0.46×0.28×0.14	0.41×0.37×0.29	0.39×0.17×0.09
Scan type/range θ/deg	ω/3.16—26.39	ω/2.84—26.37	ω/3.15—28.29	ω/2.77—26.39	ω/2.66—26.38	ω/2.69—26.39
Ranges of measured reflections	$-6 \le h \le 3$, $-20 \le k \le 17$, $-26 \le l \le 24$	$-5 \le h \le 6$, $-14 \le k \le 18$, $-33 \le l \le 31$	$-7 \le h \le 9$, $-22 \le k \le 22$, $-24 \le l \le 24$	$-37 \le h \le 48$, $-9 \le k \le 11$, $-17 \le l \le 17$	$-12 \le h \le 19$, $-21 \le k \le 16$, $-11 \le l \le 11$	$-19 \le h \le 14$, $-18 \le k \le 20$, $-11 \le l \le 10$
Number of measured reflections	5751	9015	12221	11313	8453	9413
Number of independent reflections (R_{int})	3379 (0.0408)	2322 (0.0414)	4965 (0.0389)	4940 (0.0305)	4606 (0.0421)	4585 (0.1824)
Number of reflections with $I > 2\sigma(I)$	1681	1309	3451	897	2411	1773
R Factors on $I > 2\sigma(I)$	$R_1 = 0.0407$, $wR_2 = 0.0587$	$R_1 = 0.0319$, $wR_2 = 0.0679$	$R_1 = 0.0325$, $wR_2 = 0.0694$,	$R_1 = 0.0408$, $wR_2 = 0.0784$	$R_1 = 0.0581$, $wR_2 = 0.1371$	$R_1 = 0.0571$, $wR_2 = 0.0729$
on all reflections	$R_1 = 0.1024$, $wR_2 = 0.0644$	$R_1 = 0.0608$, $wR_2 = 0.0705$	$R_1 = 0.0571$, $wR_2 = 0.0744$	$R_1 = 0.1084$, $wR_2 = 0.0784$	$R_1 = 0.1271$, $wR_2 = 0.1580$	$R_1 = 0.1797$, $wR_2 = 0.0830$
Goodness-on-fit on F^2	1.003	1.007	1.001	1.011	1.005	1.010
Residual electron density /e • Å^3, ρ_{min}/ρ_{max}	−0.160/0.172	−0.121/0.136	−0.151/0.137	−0.199/0.192	−0.375/0.240	−0.183/0.236

potentially possible reaction centers is taken into account and selection is performed by the lowest energy states without the conditions of inclusion of each space group, the number of hypothetical homochiral packings would considerably be shortened, which is demonstrated in the diagram (Fig. 11).

As a whole, among 360 generated packings in various space groups, the probability of approaching the centers $C_\alpha...C_\beta$ and/or $C_{\alpha'}...C_{\beta'}$ at distances that do not exceed 3.8 Å is observed only for 42 structures, and 28 such structures are generated for molecules **8b**. Note for comparison that nine packings were found for molecules **5**, and five packings in which $D_{C_\alpha...C_\beta} < 3.8$ Å were found for compound **6**. No structures with this approaching of potential reaction centers were isolated for molecules **8a**.

According to the simulation results for compound **8b**, there are significantly more probable states in which the interatomic distances $C_\alpha...C_\beta$ decrease and the crystal lattice energies are simultaneously low compared to other compounds. The shortest distances of this type for structure **8b** are 3.570 and 3.550 Å at the corresponding values of the lattice energy equal to −225.0 and −224.0 kJ mol^{-1}. The shortest $D_{C_\alpha...C_\beta}$ distance for structure **8a** is 3.814 Å; however, it is observed for the structure with a comparatively high lattice energy of −173.7 kJ mol^{-1}. The result of packing simulation for structure **8** in the conformational state corresponding to the total energy minimum of an isolated molecule characterized by a substantially bent shape does not allow one to observe the probability of approaching of the reaction centers by less than 4.0 Å.

Thus, the simulation results indicate that **8b** is the most probable structure for which PCA can be observed in the crystal phase. In the most part of modeled molecular packings of this compound, both the energy (thermo-

Table 3. Selected model molecular packings of compounds **5**—**8** with the minimum value of lattice energy (E)

Compound	Space group	$-E$/kJ mol^{-1}
5	$C2/c$	167.2
	$P\bar{1}$	177.34
	$P2_1$	178.81
	$P2_1/c$	185.05
	$P2_12_12_1$	183.86
	$Pbca$	165.91
6	$C2/c$	176.16
	$P\bar{1}$	184.84
	$P2_1$	194.11
	$P2_1/c$	194.86
	$P2_12_12_1$	201.87
	$Pbca$	178.74
7	$C2/c$	197.62
	$P\bar{1}$	212.13
	$P2_1$	199.7
	$P2_1/c$	214.03
	$P2_12_12_1$	201.18
	$Pbca$	195.26
8a	$C2/c$	189.15
	$P\bar{1}$	217.51
	$P2_1$	220.32
	$P2_1/c$	224.32
	$P2_12_12_1$	222.89
	$Pbca$	197.64
8b	$C2/c$	216.73
	$P\bar{1}$	230.02
	$P2_1$	207.7
	$P2_1/c$	225.01
	$P2_12_12_1$	208.34
	$Pbca$	213.39

dynamic) and geometrical control of approaching the reaction centers is provided predominantly in centrosymmetric dimers. In addition, the simulation data show that the most significant factor determining reaction center approaching in crownophanes **5**—**8**, under the fulfilled condition of thermodynamic preference of the considered types of packings, is the shape of the molecule: stabilization of comparatively planar fragments of π-systems in crystal. The possibility of reaction center approaching decreases sharply with a change in the conformational state of the structure leading to a decrease in planarity of the molecule.

Photochemical behavior of *E*,*E*-isomers 5—8 in the solid phase. As mentioned above, all condensation products **5**—**8** were mixtures of *E*,*E*- and *E*,*Z*-isomers. Prior to studies of photochemical transformations in single crystals and X-ray diffraction analyses and after chromatographic purification and recrystallization from acetonitrile or pyridine solutions, all crystalline samples studied were checked to purity and the absence of impurities (in particular, *E*,*Z*-isomers) by NMR spectroscopy. However, during the X-ray diffraction analysis of single crystal **8b** at 130(2) we found that the peaks corresponding to photoadduct **9** along the peaks of spatial electron density corresponding to compound **8b**, (Scheme 2). According to the data obtained for freshly prepared crystals **8b**, the ratio of occupancies of positions of atoms in crownophane **8b** and dimerization product **9** is 0.9/0.1 (*i.e.*, it is almost at the resolution level of the method). According to the X-ray diffraction results, the optimal[2,42] (3.5 Å) approach of photosensitive groups CH=CH in intermolecular sandwiches capable of undergoing photodimerization reactions is observed in crystals of modification **8b**. The presence of a photoadduct impurity in the corresponding crystal **8b** can be explained exclusively by photochemical transformations due to light irradiation of the crystals inevitable for X-ray diffraction analysis. Similar changes in crystals with the formation of photoadducts during X-ray diffraction studies were observed earlier for the chalcone podands as well.[41]

Scheme 2

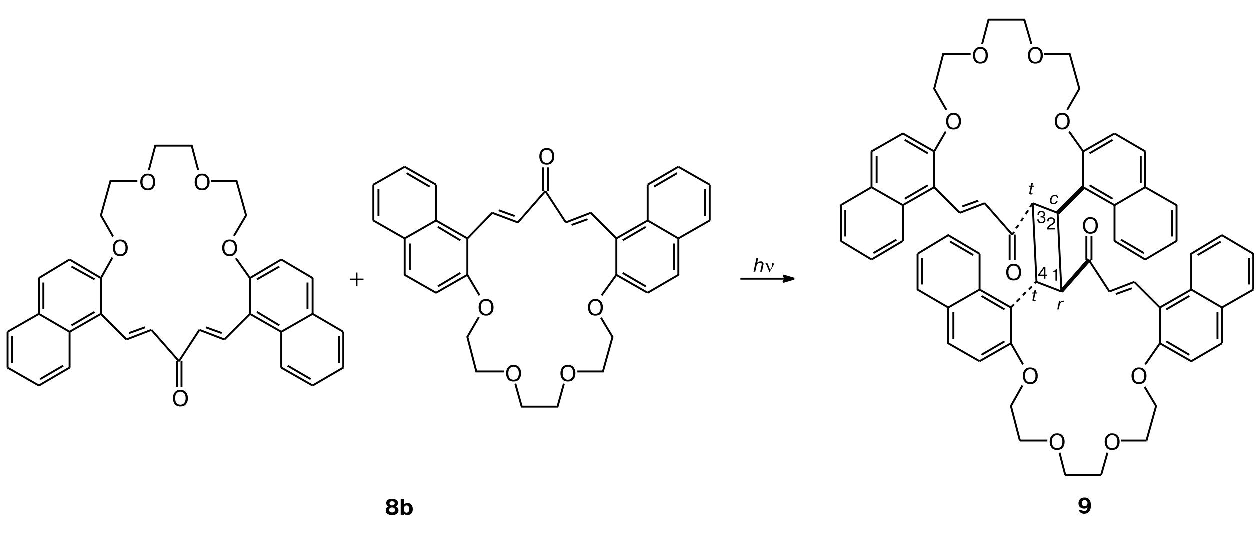

8b **9**

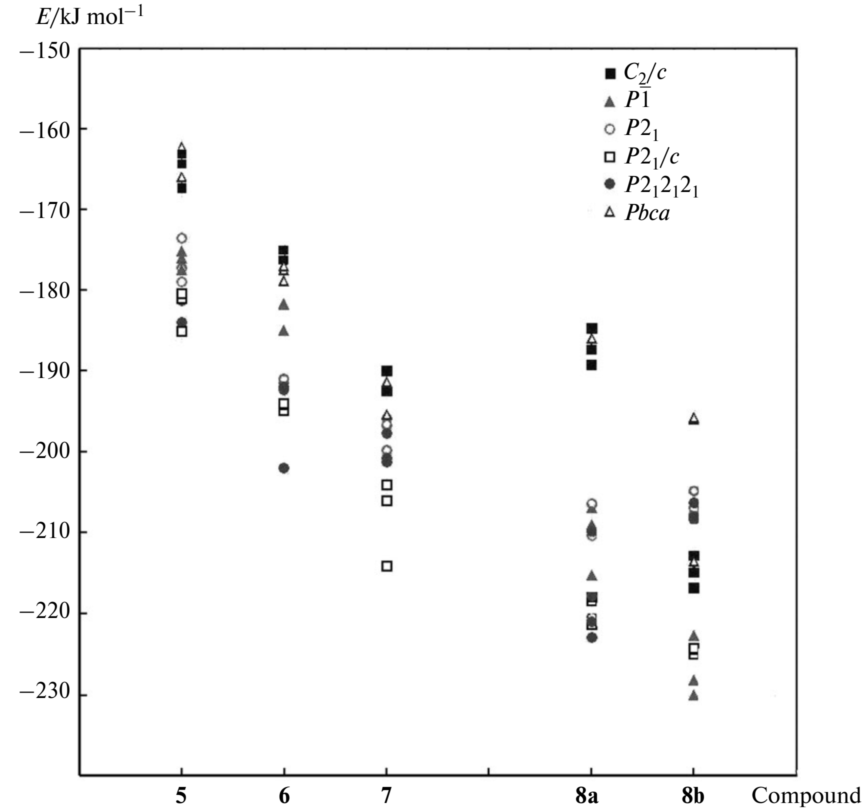

Fig. 10. Lattice energy distribution of molecular packings for triples of the lowest-energy packings of each of compounds **5**—**8**.

In turn, as sample **8b** is irradiated with non-filtered light from a mercury lamp (125 W), the occupancy of positions of product **9** in the single crystal increases. According to the X-ray diffraction data, the ratio **8b**/**9** was 0.2/0.8 for the sample irradiated for 18—20 h at 25 °C, *i.e.*, the crystal is formed predominantly by the dimerization product. The residual occupancy of positions corresponding to crownophanes **8b** can be explained, first, by the incompleteness of the dimerization process, which requires a longer irradiation time, and by a possible reversibility of the transformation of **8b** into **9** (especially under the conditions of the action of ionizing radiation in X-ray diffraction experiment). Indeed, after irradiation for a week, no signals of protons of the starting compound **8b** were observed in the ^{1}H NMR spectra of the samples. Therefore, the impurity of unreacted molecules **8b** does not exceed 1—3%.

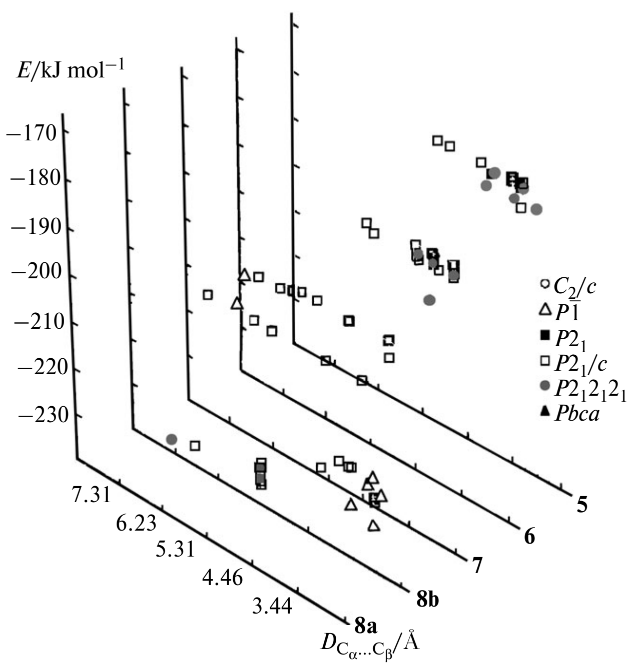

Fig. 11. Distribution of lowest-energy model structures **5**—**8** with allowance for the distance between the potential reaction centers.

Thus, the X-ray diffraction data for the irradiated single crystals indicates that the PCA reaction occurs in the whole sample bulk according to the single crystal—single crystal type with retention of the crystal structure (see Scheme 2, Fig. 12). The insignificant changes in the geometrical parameters of centrosymmetric sandwich dimers **8b** due to photolysis with the formation of cyclobutane-containing crownophane **9** are directly related to the presence of loose zones (oxyethylene fragments) around the excimeric transition complex and intermolecular π-stacking interaction of the naphthyl substituents that prevents substantial conformational changes in the reacting dimer (see Figs 9, 12, and 13).

The four-membered cycle of a molecule of crownophane **9** with the α-truxillic type of isomerism[3] is rigidly planar. In cyclobutane the C(11)—C(12) (1.541(1) Å) and C(11)—C(12A) (1.612(1) Å) bond lengths differ insignificantly, as the conjugated angles C(11A)—C(12A)—C(11) and C(12)—C(11)—C(12A) (90.07(1) and 89.93(1)°, respec-

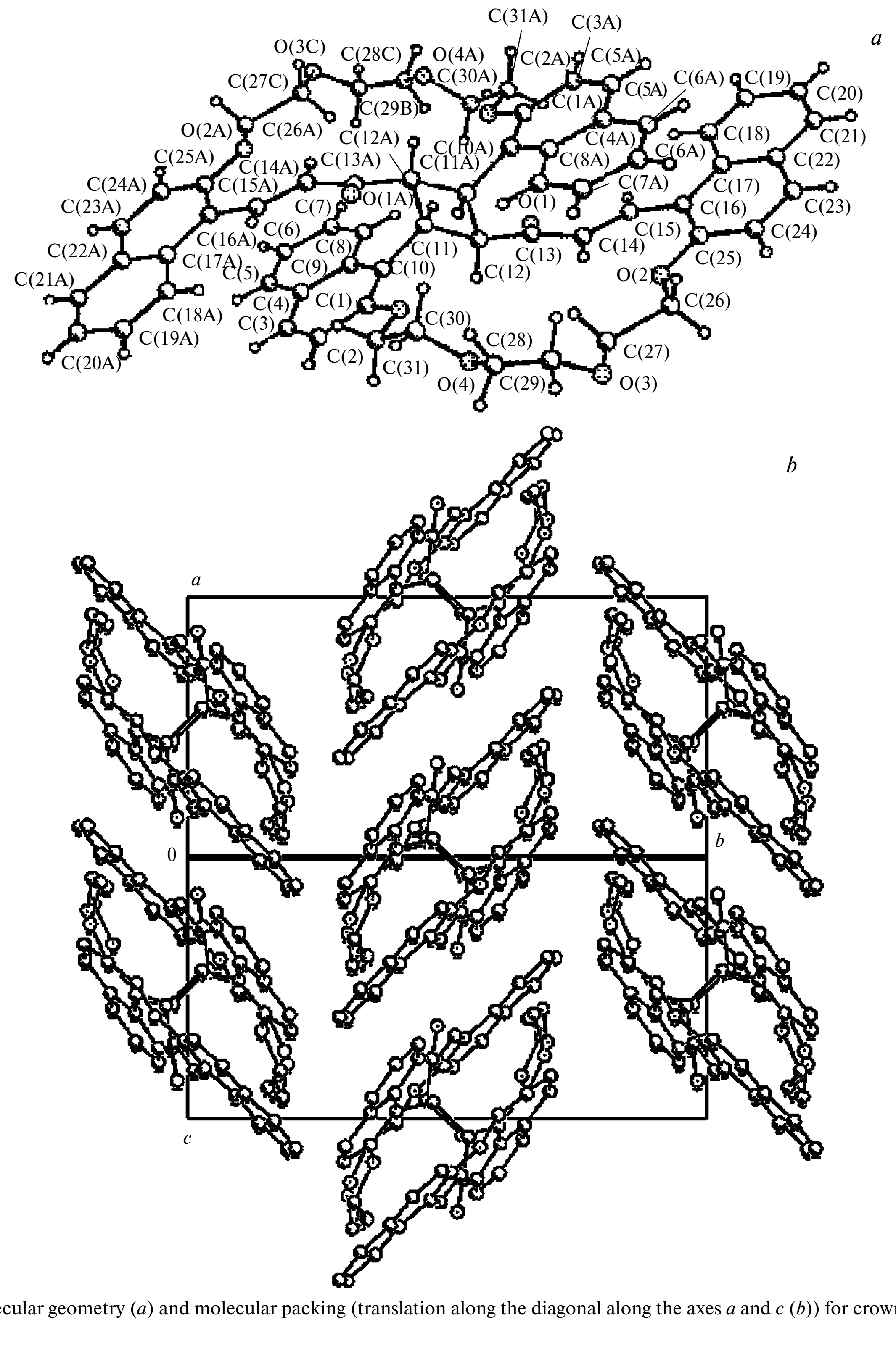

Fig. 12. Molecular geometry (*a*) and molecular packing (translation along the diagonal along the axes *a* and *c* (*b*)) for crownophane **9**.

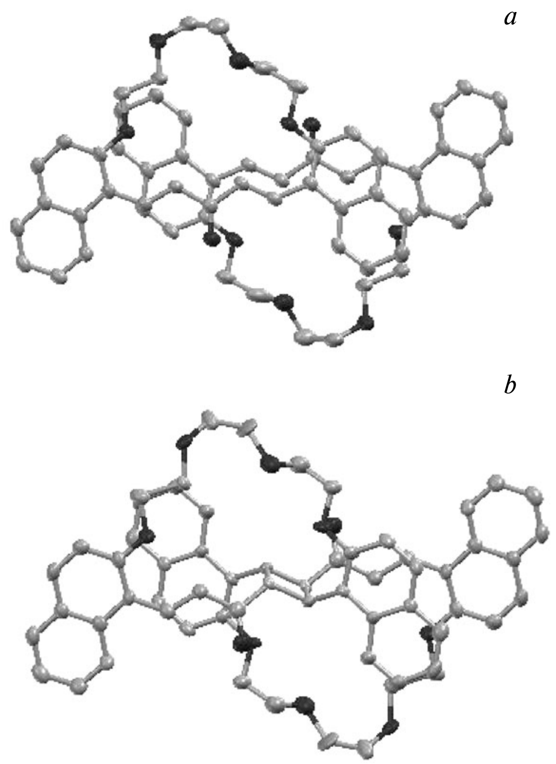

Fig. 13. Geometry of dimer **8b** before (*a*) and after irradiation (*b*) of crownophane **9** with non-filtered light of a mercury lamp.

tively). The torsion angles C(10)—C(11)—C(12)—C(13) and C(10)—C(11)—C(12A)—C(13A) are 114.41(2) and 2.62(2)°, respectively.

Along with X-ray diffraction, the photoinduced changes in single crystals of crownophane **8b** associated with the partial disappearance of the chromophoric fragments were confirmed by a decrease in the light absorption maximum (λ = 450 nm) in the UV (DRA) spectra with the simultaneous hypsochromic shift of the absorption in the wavelength region 350—450 nm (Fig. 14). In the IR spectra (DRA) the formation of the cyclobutane fragment was determined from the shift of the absorption band maximum of stretching vibrations of the carbonyl group to the high-frequency region by 19 cm^{-1} (1673 cm^{-1} (C=O)) and the appearance of new absorption band maxima at 2924 and 2910 cm^{-1} (region of stretching vibrations of C—H bonds).[41] We earlier observed similar changes in single crystals for chalcone podands. However, unlike the latter, insignificant redistributions of the absorption band intensities in the region of bending vibrations of the C—O—C bonds of the oxyethylene fragment at 1139—1188 cm^{-1} indicate slight conformational changes during PCA in molecules **8b** (see Fig. 14).

In the ^{1}H NMR spectra, protons of the cyclobutane fragment of photoadduct **9** form a symmetrical spin system of the AA´XX´ type characteristic of the *rctt*-isomer (Fig. 15), which can be considered in the first-order approximation as two doublets of doublets with the chemical shifts 6.20 and 4.94 ppm and SSCC $^3J_{AX} = {}^3J_{A'X'}$ = 12.0 Hz and $^3J_{A'X} = {}^3J_{AX'}$ = 8.0 Hz.

On going to compounds **5—7**, the intermolecular distances between the photosensitive groups CH=CH increase to 4.8—6.9 Å due to topotactic control of the molecular lattices and, hence, the occurrence of PCA in crystals of these crownophanes is poorly probable. However, another type of photochemical transformations in the solid phase is possible for olefins: *E*—*Z*-isomerization. Similar processes were observed earlier for acyclic analogs of

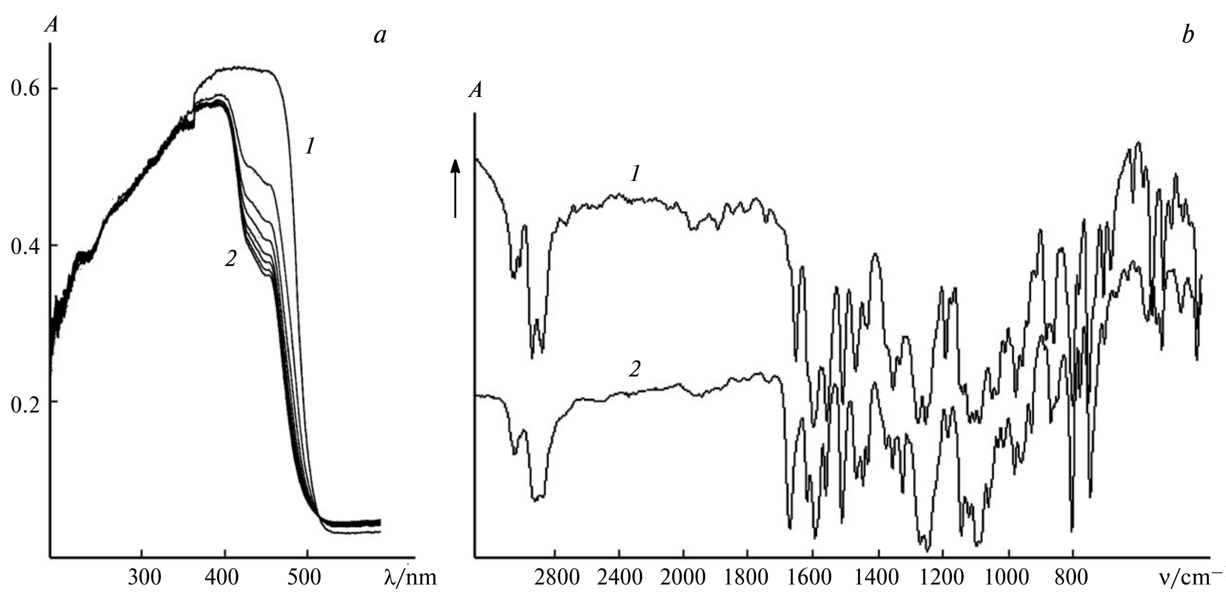

Fig. 14. (*a*) UV absorption spectra (DRA) of compound **8b** upon visible light irradiation: the starting compound (*1*), the PCA product (*2*); (*b*) IR absorption spectra (DRA) of crownophane **8b** (*1*) and the cyclobutane-containing adduct **9** (*2*).

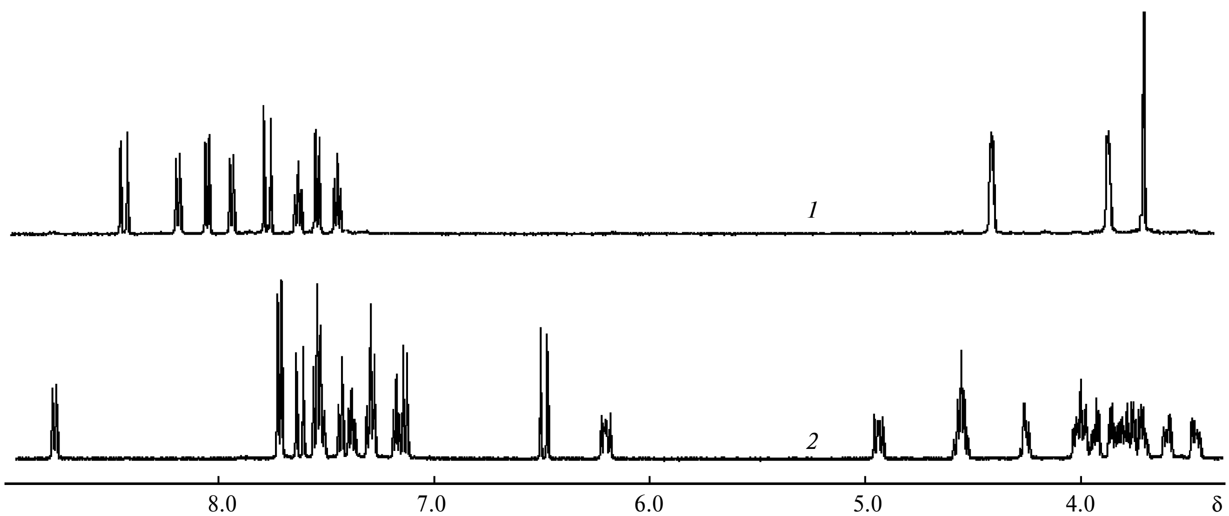

Fig. 15. ^{1}H NMR spectra (400 MHz, DMSO-d_6) of compound **8b** before irradiation (*1*) and product **9** after irradiation with non-filtered light from a mercury lamp (125 W) (*2*).

crownophanes (chalcone podands) and it was assumed that *E—Z*-isomerization occurred probably on defects and/or faces of crystals involving one of terminal chalcone groups in the photochemical reaction. This group is not bound by stacking interactions and is partially liberated from the influence of the adjacent environment.[41] It was marked that the conjugated group Ph—C=O with the CH=CH fragment of chalcone podands favors an increase in the singlet-triplet conversion constant (sensibilizing ability) and, hence, an increase in the probability of photoinduced *E—Z*-isomerization.[47]

It was found by NMR spectroscopy that during photolysis molecules in crystals of compounds **5—7** can undergo *E—Z*-isomerization of the CH=CH bond to form stereoisomers **5a—7a** (Scheme 3, Fig. 16).

The interpretation of the ^{1}H NMR spectroscopic data for the starting and irradiated crystals of compounds **5—7** suggests isomerization analogous to that observed earlier[41] for the chalocone podands of only one of the —CH=CH— groups of the pentadienone fragment of crownophanes during photochemical transformations. In particular, the spectra of crownophane **5** contain signals of the α,β-protons of the CH=CH group in the *Z*-configuration at δ 6.27 and 7.10 as two doublets with the SSCC 12.7 Hz and also signals at δ 6.62 and 7.80 of the α,β-protons of the second fragment in the *E*-configuration with the SSCC 16.8 Hz (see Fig. 16).

Thus, the X-ray diffraction studies of molecular packings of diarylideneacetonyl crownophanes **5—8** confirm the earlier formulated thesis about the ability of crown ethers[33—39] and their acyclic analogs[40,41] (podands) with photochromic side groups to enter into the PCA reaction in crystals packed predominantly as centrosymmetrical dimers. According to the experimental data, topotactic control of photosensitive center approaching takes place for this type of packing. In the case of diarylideneacetonyl crownophanes, the introduction of naphthyl substituents into the chromophoric fragment along with the "planar" geometry is the key factor in the formation of the corresponding centrosymmetric dimers in the solid phase.

Scheme 3

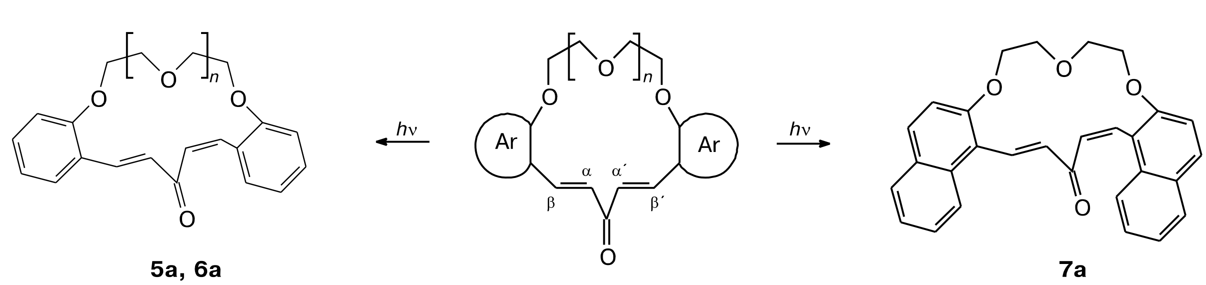

5, **6:** *n* = 1, 2. Ar = Ph; **7:** *n* = 1, Ar is naphthyl.

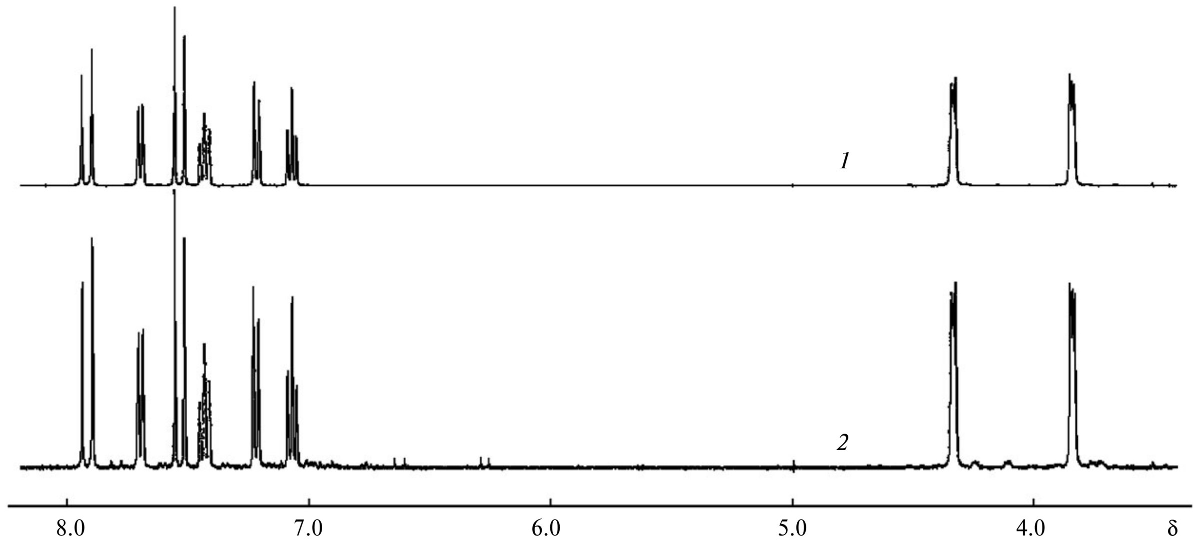

Fig. 16. ^{1}H NMR spectra (400 MHz, DMSO-d_6) of compound **5** before (*1*) and after irradiation with non-filtered light from a mercury lamp (125 W) for 12 h (*2*).

In turn, the concerted action of the conformationally mobile oligooxyethylene fragment and naphthyl substituents in molecules provides the stereospecific PCA reaction to occur in crystals of modification **8b** by the single crystal—single crystal type.

Experimental

IR spectra were recorded on a Spectrum One FTIR spectrometer (Perkin—Elmer) using a diffuse reflectance sampling accessory (DRA). UV spectra were measured on a UV-2401 PC spectrometer (Shimadzu) using an integrating sphere attachment. ^{1}H and ^{13}C NMR spectra were recorded in DMSO-d_6 solutions on Bruker DRX-400 and Bruker AV-500 instruments with working frequencies of 400.1, 500.1 and 100.6, 125.8 MHz, respectively, using Me_4Si and DMSO-d_6 (δ_C 39.5) as internal standards. The complete assignment of signals in the ^{1}H and ^{13}C NMR spectra was performed using 2D NOESY, HSQC, and HMBC experiments. Melting points were determined on a Boetius microheating stage. Thin-layer chromatography was carried out on Silufol-254 plates. The points were developed with iodine vapors.

Synthesis of diarylideneacetonyl crownophanes 5—8. A mixture of formyl podand[40] **1—4** (0.96 mmol) and acetone (2.88 mmol) in ethanol (50 mL) was heated in a flask to 65—70 °C and magnetically stirred at this temperature for 30 min. Then a 20% ethanolic solution (3 mL) of KOH was added, and stirring was continued with gradual cooling of the reaction mixture to ~20 °C. The solution was additionally stored in the dark for 12 h. Water was added to the reaction mixture, and the precipitate formed was filtered off by washing with several portions of water on the filter. Products **5—8** were purified and separated using column chromatography (SiO_2), eluting with an ethyl acetate—hexane (1 : 1) mixture. Compounds **5—8** were recrystallized from an acetonitrile solution.

(16*E*,19*E*)-Dibenzo[*h*,*o*][1,4,7]trioxacyclohexadeca-16,19-dien-18-one (5). The yield was 38%, m.p. 172—174 °C. ^{1}H NMR (400 MHz), δ: 3.84 (m, 4 H, H(7), H(9)); 4.33 (m, 4 H, H(6), H(10)); 7.07 (ddd, 2 H, H(2), H(14), J = 7.6 Hz, J = 7.4 Hz, J = 0.8 Hz); 7.22 (dd, 2 H, H(4), H(12), J = 8.3 Hz, J = 0.8 Hz); 7.43 (ddd, 2 H, H(3), H(13), J = 8.3 Hz, J = 7.4 Hz, J = 1.6 Hz); 7.54 (d, 2 H, H(17), H(19), J = 16.4 Hz); 7.70 (dd, 2 H, H(1), H(15), J = 7.6 Hz, J = 1.6 Hz); 7.92 (d, 2 H, H(16), H(20), J = 16.4 Hz). ^{13}C NMR (100 MHz), δ: 69.15 (C(6), C(10)); 69.43 (C(7), C(9)); 114.91 (C(4), C(12)); 121.74 (C(2), C(14)); 124.28 (C(15a), C(20a)); 126.03 (C(17), C(19)); 130.60 (C(1), C(15)); 131.79 (C(3), C(13)); 138.72 (C(16), C(20)); 157.85 (C(4a), C(11a)); 190.17 (C(18)). IR (DRA), ν/cm^{-1}: 569, 611; 728, 756, 781 (arom.); 834, 890, 923, 943; 1016, 1043, 1062, 1102, 1123, 1165, 1184, 1221, 1257 (ν_s, ν_{as}, C_{arom}—O—C_{alk}, C_{alk}—O—C_{alk}); 1272, 1313, 1333, 1457, 1482; 1569, 1588 (C=C); 1645 (C=O); 2827, 2875, 2901, 2937, 2988 (C_{alk}—H); 3033, 3052, 3072 (C_{arom}—H). Found (%): C, 74.93; H, 6.03. $C_{21}H_{20}O_4$. Calculated (%): C, 75.00; H, 5.95.

(19*E*,22*E*)-Dibenzo[*k*,*r*][1,4,7,10]tetraoxacyclononadeca-19,22-dien-21-one (6). The yield was 27%, m.p. 100—102 °C. ^{1}H NMR (400 MHz), δ: 3.71 (s, 4 H, H(9), H(10)); 3.87 (m, 4 H, H(7), H(12)); 4.25 (m, 4 H, H(6), H(13)); 7.02 (ddd, 2 H, H(2), H(17), J = 7.6 Hz, J = 7.4 Hz, J = 1.0 Hz); 7.12 (d, 2 H, H(4), H(15), J = 8.1 Hz); 7.41 (ddd, 2 H, H(3), H(16), J = 8.1 Hz, J = 7.4 Hz, J = 1.7 Hz); 7.50 (d, 2 H, H(20), H(22), J = 15.9 Hz); 7.59 (dd, 2 H, H(1), H(18), J = 7.6 Hz, J = 1.7 Hz); 7.64 (d, 2 H, H(19), H(23), J = 15.9 Hz). ^{13}C NMR (100 MHz), δ: 67.30 (C(6), C(13)); 68.48 (C(7), C(12)); 70.01 (C(9), C(10)); 112.19 (C(4), C(15)); 120.79 (C(2), C(17)); 122.88 (C(18a), C(23a)); 128.44 (C(20), C(22)); 131.63 (C(3), C(16)); 133.78 (C(1), C(18)); 139.70 (C(19), C(23)); 158.13 (C(4a), C(14a)); 189.55 (C(21)). IR (DRA), ν/cm^{-1}: 568, 613; 716, 746, 788 (arom.); 830, 852, 889, 914, 943, 992; 1058, 1090, 1122, 1162, 1196, 1237, 1259 (ν_s, ν_{as}, C_{arom}—O—C_{alk}, C_{alk}—O—C_{alk}); 1301, 1338, 1361, 1376, 1445, 1455, 1493; 1569, 1615 (C=C); 1666 (C=O); 2767, 2872, 2925 (C_{alk}—H); 3022, 3047, 3070 (C_{arom}—H). Found (%): C, 72.67; H, 6.59. $C_{23}H_{24}O_5$. Calculated (%): C, 72.63; H, 6.32.

(20*E*,23*E*)-Dinaphtho[2,1-*h*:1´,2´-*o*][1,4,7]trioxacyclohexadeca-20,23-dien-22-one (7). The yield was 42%, m.p. 232—234 °C. ^{1}H NMR (500.1 MHz), δ: 3.89 (m, 4 H, H(9), H(11)); 4.51 (m, 4 H, H(8), H(12)); 7.48 (ddd, 2 H, H(3), H(17), *J* = 8.1 Hz, *J* = 6.9 Hz, *J* = 0.8 Hz); 7.60 (d, 2 H, H(6), H(14), *J* = 9.2 Hz); 7.64 (ddd, 2 H, H(2), H(18), *J* = 8.6 Hz, *J* = 6.9 Hz, *J* = 1.4 Hz); 7.70 (d, 2 H, H(21), H(23), *J* = 16.4 Hz); 7.97 (dd, 2 H, H(4), H(16), *J* = 8.1 Hz, *J* = 1.4 Hz); 8.07 (d, 2 H, H(5), H(15), *J* = 9.2 Hz); 8.27 (dd, 2 H, H(1), H(19), *J* = 8.6 Hz, *J* = 0.8 Hz); 8.48 (д, 2 H, H(20), H(24), *J* = 16.4 Hz). ^{13}C NMR (125.8 MHz), δ: 69.34 and 69.35 (C(8), C(9), C(11), C(12)); 115.65 (C(6), C(14)); 117.47 (C(19b), C(24a)); 122.78 (C(1), C(19)); 124.19 (C(3), C(17)); 127.77 (C(2), C(18)); 128.82 (C(4), C(16)); 129.10 (C(4a), C(15a)); 129.35 (C(21), C(23)); 131.85 (C(19a), C(24b)); 132.11 (C(5), C(15)); 135.62 (C(20), C(24)); 156.13 (C(6a), C(13a)); 190.16 (C(22)). IR (DRA), ν/cm^{-1}: 559, 663, 696; 740, 757 (arom.); 808, 818, 867, 889, 932, 962, 978, 997; 1058, 1075, 1094, 1122, 1163, 1185, 1210, 1254, 1269, 1287 (ν_s, ν_{as}, C_{arom}—O—C_{alk}, C_{alk}—O—C_{alk}); 1315, 1348, 1377, 1432, 1445, 1455, 1469, 1510; 1558, 1582, 1608 (C=C); 1642 (C=O); 2743, 2804, 2825, 2855, 2875, 2909, 2931, 2951, 2988 (C_{alk}—H); 3020. 3046, 3057, 3070 (C_{arom}—H). Found (%): C, 79.99; H, 5.47. $C_{29}H_{24}O_4$. Calculated (%): C, 79.81; H, 5.50.

(23*E*,26*E*)-Dinaphtho[2,1-*k*:1´,2´-*r*][1,4,7,10]tetraoxacyclononadeca-23,26-dien-25-one (8). The yield was 25%, m.p. 191—193 °C (modification **8a**), m.p. 204—206 °C (modification **8b**). ^{1}H NMR (400 MHz), δ: 3.72 (s, 4 H, H(11), H(12)); 3.88 (m, 4 H, H(9), H(14)); 4.42 (m, 4 H, H(8), H(15)); 7.46 (ddd, 2 H, H(3), H(20), *J* = 8.0 Hz, *J* = 6.9 Hz, *J* = 1.0 Hz); 7.55 (d, 2 H, H(6), H(17), *J* = 9.1 Hz); 7.64 (ddd, 2 H, H(2), H(21), *J* = 8.6 Hz, *J* = 6.9 Hz, *J* = 1.2 Hz); 7.79 (d, 2 H, H(24), H(26), *J* = 15.6 Hz); 7.94 (dd, 2 H, H(4), H(19), *J* = 8.0 Hz, *J* = 1.2 Hz); 8.06 (d, 2 H, H(5), H(18), *J* = 9.1 Hz); 8.20 (d, 2 H, H(1), H(22), *J* = 8.6 Hz); 8.45 (d, 2 H, H(23), H(27), *J* = 15.6 Hz). ^{13}C NMR (100 MHz), δ: 67.70 (C(8), C(15)); 68.73 (C(9), C(14)); 69.87 (C(11), C(12)); 114.07 (C(6), C(17)); 115.00 (C(22b), C(27a)); 122.01 (C(1), C(22)); 123.90 (C(3), C(20)); 127.84 (C(2), C(21)); 128.49 (C(4a), C(18a)); 128.90 (C(4), C(19)); 131.20 (C(24), C(26)); 132.39 (C(5), C(18)); 133.01 (C(22a), C(27b)); 133.87 (C(23), C(27)); 156.95 (C(6a), C(16a)); 189.60 (C(25)). IR spectrum of modification **8a** (DRA), ν/cm^{-1}: 562, 654, 681; 705, 735, 748, 803 (arom.); 841, 866, 894, 948, 989; 1033, 1049, 1093, 1105, 1117, 1148, 1246, 1262 (ν_s, ν_{as}, C_{arom}—O—C_{alk}, C_{alk}—O—C_{alk}); 1343, 1356, 1380, 1449, 1469, 1489, 1511; 1556, 1602 (C=C); 1656 (C=O); 2870, 2912 (C_{alk}—H); 3065 (C_{arom}—H). IR spectrum (DRA) of modification **8b**, ν/cm^{-1}: 555, 683; 706, 751, 781, 800 (arom.); 859, 882, 956, 976, 1009; 1033, 1049, 1088, 1104, 1119, 1139, 1254, 1278 (ν_s, ν_{as}, C_{arom}—O—C_{alk}, C_{alk}—O—C_{alk}); 1335, 1354, 1433, 1469, 1510; 1559, 1600 (C=C); 1654 (C=O); 2732, 2879, 2941 (C_{alk}—H); 3017, 3049 (C_{arom}—H). Found (%): C, 77.63; H, 5.82. $C_{31}H_{28}O_5$. Calculated (%): C, 77.50; H, 5.83.

Photochemical transformations in single crystals of crownophanes 5—8 and solid-phase synthesis of cyclobutane-containing crownophane *rctt*-9. Single crystals of crownophanes **5—8** were irradiated with non-filtered light from a mercury lamp (125 W) in a setup with thermal filters and air cooling to 25 °C from a distance of 10 cm for 12—18 h. The reaction course was monitored using IR spectra (DRA), UV spectra (DRA), and ^{1}H NMR spectra. The ratio of *E*,*E*/*E*,*Z*-isomers in the reaction mixture was estimated by comparing integral intensities of signals from α,β-protons in the ^{1}H NMR spectra. Photolysis product **9** was purified by recrystallization from DMF.

Crownophane *rctt*-9, m.p. >350 °C. ^{1}H NMR (500.1 MHz), 120 °C, δ: 3.47 (m, 2 H, OCH_2); 3.60 (m, 2 H, OCH_2); 3.68—3.91 (m, 8 H, OCH_2); 3.91 —4.03 (m, 6 H, OCH_2); 4.26 (m, 2 H, OCH_2); 4.56 (m, 4 H, OCH_2); 4.94 and 6.20 (both dd, 2 H each, CH—CH, *J* = 12.0 Hz, *J* = 8.0 Hz); 6.49 (d, 2 H, CH=CH, *J* = 16.2 Hz); 7.13 (d, 2 H, Ar, *J* = 9.0 Hz); 7.18 (ddd, 2 H, Ar, *J* = 7.5 Hz, *J* = 7.2 Hz, *J* = 0.6 Hz); 7.24—7.31 (m, 4 H, Ar); 7.38 (ddd, 2 H, Ar, *J* = 8.4 Hz, *J* = 6.8 Hz, *J* = 1.3 Hz); 7.43 (d, 2 H, Ar, *J* = 8.4 Hz); 7.50—7.56 (m, 6 H, Ar); 7.62 (d, 2 H, CH=CH, *J* = 16.2 Hz); 7.72 (d, 4 H, Ar, *J* = 8.8 Hz); 8.76 (d, 2 H, Ar, *J* = 8.6 Hz). IR (DRA), ν/cm^{-1}: 525, 569; 746, 778, 803 (arom.); 848, 868, 927, 959, 980; 1031, 1060, 1098, 1121, 1144, 1250, 1271 (ν_s, ν_{as}, C_{arom}—O—C_{alk}, C_{alk}—O—C_{alk}); 1326, 1355, 1376, 1433, 1447, 1468, 1512; 1561, 1595 (C=C); 1620, 1673 (C=O); 2873, 2910, 2938 (C_{alk}—H); 3014, 3040 (C_{arom}—H). Found (%): C, 77.63; H, 5.82. $C_{62}H_{56}O_{10}$. Calculated (%): C, 77.50; H, 5.83.

X-ray diffraction study. Crystals of crownophanes **5** and **6** were obtained by the slow evaporation of the solution in acetonitrile (crownophanes **7** and **8** were evaporated in acetonitrile (modification **8b**) or pyridine (modification **8a**)). X-ray diffraction analysis was performed on an Xcalibur 3 automated diffractometer with a CCD detector (Mo-Kα radiation, λ = 0.71073 Å, graphite monochromator, ω/2θ scan mode, scan increment 1°) at 295(2) K (compounds **5—7** and **8a**) or 130(2) K (compounds **8b** and **9**). A set of reflections was obtained and processed using the CrysAlis program package.[48] The structures were determined by a direct method and refined by full-matrix least squares first in the isotropic approximation and then in the anisotropic approximation on F^2 for all non-hydrogen atoms using the SHELXS-97 and SHELXL-97 programs.[49] Some hydrogen atoms were revealed in the difference synthesis and included in the isotropic approximation, and some atoms were placed in geometrically calculated positions and refined using the riding model. The X-ray diffraction experimental data for structures **5—9** were deposited with the Cambridge Crystallographic Data Centre (CCDC Nos 822 568 (**5**), 822 569 (**6**), 822 567 (**7**), 822 566 (**8a**), 822 565 (**8b**), and 822 579 (**9**). Copies of the data can be received free of charge at The Director, CCDC, 12 Union Road, Cambridge CB2 1EZ, UK [fax: (+44)-1223/336-033; e-mail: deposit@ccdc.cam.ac.uk].

Studies using computation methods. Crystal packings for the studied structures of crownophanes **5—8** were modeled using the Opix algorithm.[50] The algorithm makes it possible to generate molecular packings of crystals in six space groups ($P\bar{1}$, $P2_1$, $P2_12_12_1$, $P2_1/c$, $C2/c$, and *Pbca*) in which the predominant part of organic compounds crystallize.[51,52] The X-ray diffraction data for which the positions of hydrogen atoms were pre-normalized served as the initial data for the reproduction of the random set of probable crystal packings. Since the most part of the studied structures are conformationally mobile, we performed the full conformational analysis for isolated molecular structures **5—8** using the Ballon algorithm.[53] At the stage of selection of the most probable conformational states, geometry optimization procedures (RM1 method) were successively used by the MOPAC (see Ref. 54) and Conformers programs.[55] The most thermodynamically probable packings in each of the considered space groups characterized by the lowest calculated energies of the crystal lattices were analyzed for the closeness of the reaction centers $C_{\alpha}...C_{\beta}$ and/or $C_{\alpha'}...C_{\beta'}$ of the potentially possible photoinduced cycloaddition process. A total of 360 generated structures of molecular crystal packings was considered.[56,57]

This work was financially supported by the Presidium of the Ural Branch of the Russian Academy of Sciences (Grants 09-I-3-2004, 09-P-3-2001, 09-T-3-1024, and 09-I-3-2004).

References

1. J.-M. Lehn, *Supramolecular Chemistry. Concepts and Perspectives*, VCH, Weinheim, 1995, Ch. **8**.
2. V. Ramamurthy, K. Venkatesan, *Chem. Rev.*, 1987, **87**, 433.
3. L. R. MacGillivray, G. S. Papaefstathiou, T. Friščić, D. B. Varshney, T. D. Hamilton, *Top. Curr. Chem.*, 2005, **248**, 201.
4. M. D. Cohen, G. M. Schmidt, *J. Chem. Soc.*, 1964, 1996.
5. M. D. Cohen, G. M. Schmidt, F. I. Sonntag, *J. Chem. Soc.*, 1964, 2000.
6. G. M. Schmidt, *J. Chem. Soc.*, 1964, 2014.
7. M. Hasegawa, K. Saigo, T. Mori, H. Uno, M. Nohara, H. Nakanishi, *J. Am. Chem. Soc.*, 1985, **107**, 2788.
8. C.-M. Chung, A. Kunita, K. Hayashi, F. Nakamura, K. Saigo, M. Hasegawa, *J. Am. Chem. Soc.*, 1991, **113**, 7316.
9. N. M. Peachey, C. J. Eckhardt, *J. Am. Chem. Soc.*, 1993, **115**, 3519.
10. I. Turowska-Tyrk, K. Grzeniak, E. Trzop, T. Zych, *J. Solid State Chem.*, 2003, **174**, 459.
11. S.-Y. Yang, P. Naumov, S. Fukuzumi, *J. Am. Chem. Soc.*, 2009, **131**, 7247.
12. D.-K. Buèar, G. S. Papaefstathiou, T. D. Hamilton, Q. L. Chu, I. G. Georgiev, L. R. MacGillivray, *Eur. J. Inorg. Chem.*, 2007, 4559.
13. N. W. Alcock, N. Herron, T. J. Kemp, C. W. Shoppee, *J. Chem. Soc., Chem. Commun.*, 1975, 785.
14. W.-L. Nie, G. Erker, G. Kehr, R. Fröhlich, *Angew. Chem.*, 2004, **116**, 313.
15. T. K. Maji, K. Uemura, H.-C. Chang, R. Matsuda, S. Kitagawa, *Angew. Chem.*, 2004, **116**, 3331.
16. K. Hanson, N. Calin, D. Bugaris, M. Scancella, S. C. Sevov, *J. Am. Chem. Soc.*, 2004, **126**, 10502.
17. N. L. Toh, M. Nagarathinam, J. J. Vittal, *Angew. Chem.*, 2005, **117**, 2277.
18. Q. Chu, D. C. Swenson, L. R. MacGillivray, *Angew. Chem.*, 2005, **117**, 3635.
19. M. Nagarathinam, J. J. Vittal, *Angew. Chem.*, 2006, **118**, 4443.
20. J. Paradies, I. Greger, G. Kehr, G. Erker, K. Bergander, R. Fröhlich, *Angew. Chem.*, 2006, **118**, 7792.
21. J. F. Eubank, V. C. Kravtsov, M. Eddaoudi, *J. Am. Chem. Soc.*, 2007, **129**, 5820.
22. M. Nagarathinam, J. J. Vittal, *Chem. Commun.*, 2008, 438.
23. Z. Wang, S. M. Cohen, *Angew. Chem.*, 2008, **120**, 4777.
24. T. Kawamichi, T. Kodama, M. Kawano, M. Fujita, *Angew. Chem.*, 2008, **120**, 8150.
25. A. D. Burrows, C. G. Frost, M. F. Mahon, C. Richardson, *Angew. Chem.*, 2008, **120**, 8610.
26. Y. J. Zhang, T. Liu, S. Kanegawa, O. Sato, *J. Am. Chem. Soc.*, 2009, **131**, 7942.
27. D. Liu, Z.-G. Ren, H.-X. Li, J.-P. Lang, N.-Y. Li, B. F. Abrahams, *Angew. Chem., Int. Ed. Engl.*, 2010, **49**, 4767.
28. M. H. Mir, L. L. Koh, G. K. Tan, J. J. Vittal, *Angew. Chem.*, 2010, **122**, 400.
29. Y. Ito, B. Borecka, J. Trotter, J. R. Scheffer, *Tetrahedron Lett.*, **1995**, 36, 6083.
30. L. R. MacGillivray, J. L. Reid, J. A. Ripmeester, *J. Am. Chem. Soc.*, 2000, **122**, 7817.
31. L. R. MacGillivray, *Cryst. Eng. Comm.,* 2004, **6**, 77.
32. S. Yamada, N. Uematsu, K. Yamashita, *J. Am. Chem. Soc.*, 2007, **129**, 12100.
33. A. I. Vedernikov, S. P. Gromov, N. A. Lobova, L. G. Kuz´mina, Yu. A. Strelenko, J. A. K. Howard, M. V. Alfimov, *Izv. Akad. Nauk*, *Ser. Khim.*, 2005, 1896 [*Russ. Chem. Bull., Int. Ed.*, 2005, **54**, 1954].
34. L. G. Kuz´mina, O. A. Fedorova, E. N. Andryukhina, M. M. Mashura, S. P. Gromov, M. V. Alfimov, *Kristallografiya*, 2006, **51**, 467 [*Crystallogr. Repts* (*Engl. Transl.*), 2006, **51**].
35. A. I. Vedernikov, L. G. Kuz´mina, S. K. Sazonov, N. A. Lobova, P. S. Loginov, A. V. Churakov, Yu. A. Strelenko, J. A. K. Howard, M. V. Alfimov, S. P. Gromov, *Izv. Akad. Nauk*, *Ser. Khim.*, 2007, 1797 [*Russ. Chem. Bull., Int. Ed.*, 2007, **56**, 1860].
36. L. G. Kuz´mina, A. I. Vedernikov, N. A. Lobova, A. V. Churakov, J. A. K. Howard, M. V. Alfimov, S. P. Gromov, *New J. Chem.*, 2007, **31**, 980.
37. L. G. Kuz´mina, A. I. Vedernikov, S. K. Sazonov, N. A. Lobova, P. S. Loginov, J. A. K. Howard, M. V. Alfimov, S. P. Gromov, *Kristallografiya*, 2008, **53**, 460 [*Crystallogr. Repts* (*Engl. Transl.*), 2008, **53**].
38. L. G. Kuz´mina, A. I. Vedernikov, J. A. K. Howard, M. V. Almimov, S. P. Gromov, *Ross. Nanotekhnologii* [*Russian Nanotechnologies*], 2008, **3**, Nos 7—8, 32 (in Russian).
39. L. G. Kuz´mina, A. I. Vedernikov, N. A. Lobova, S. K. Sazonov, S. S. Basok, J. A. K. Howard, S. P. Gromov, *Izv. Akad. Nauk*, *Ser. Khim.*, 2009, 1161 [*Russ. Chem. Bull., Int. Ed.*, 2009, **58**, 1192].
40. I. G. Ovchinnikova, O. V. Fedorova, P. A. Slepukhin, I. A. Litvinov, G. L. Rusinov, *Kristallografiya*, 2009, **54**, 32 [*Crystallogr. Repts* (*Engl. Transl.*), 2009, **54**].
41. I. G. Ovchinnikova, O. V. Fedorova, L. G. Kuz´mina, P. A. Slepukhin, A. A. Tumashov, G. L. Rusinov, V. N. Charushin, *Izv. Akad. Nauk*, *Ser. Khim.*, 2009, 2219 [*Russ. Chem. Bull.*, *Int. Ed.*, 2009, **58,** 2288].
42. M. Hasegawa, *Chem. Rev.*, 1983, **83**, 507.
43. I. Azumaya, K. Yamaguchi, I. Okamoto, H. Kagechika, K. Shudo, *J. Am. Chem. Soc.*, 1995, **117**, 9083.
44. W. L. Meyer, P. B. Meyer, *J. Am. Chem. Soc.*, 1963, **85**, 2170.
45. S. Toyota, T. Makino, *Tetrahedron Lett.*, 2003, **44**, 7775.
46. E. Weber, J. L. Toner, I. Goldberg, F. Vögtle, D. A. Laidler, J. F. Stoddart, R. A. Bartsch, C. L. Liotta, *Crown Ethers and Analogs*, John Wiley and Sons, Chichester, 1989, Ch. **2**, p. 3.
47. F. A. Carey, R. J. Sundberg, *Advanced Organic Chemistry*, *P. A; Structure and Mechanisms, 5. Photochemistry*, Springer US, New York, 2007, **12**, 1073.
48. *CrysAlis Pro, Version 171.33.66*, Oxford Diffraction Ltd.
49. G. M. Sheldrick, *Acta Crystallogr., Sec. A*, 2008, **64**, 112.

50. A. Gavezzotti, OPiX, *A Computer Program Package for the Calculation of Intermolecular Interactions and Crystal Tnergies*, University of Milano, Milano, 2003.
51. A. Gavezzotti, *Molecular Aggregation*, Oxford University Press, New York, 2007.
52. P. M. Zorkii, P. N. Oleinikov, *Zh. Strukt. Khim.*, 2001, **42**, No. 1, 31 [*J. Struct. Chem.* (*Engl. Transl.*), 2001, **42**, No. 1].
53. M. J. Vainio, M. S. Johnson, *J. Chem. Inform. and Model.*, 2007, **47**, 2462.
54. J. J. P. Stewart, *MOPAC2009*, Stewart Computational Chemistry, Colorado Springs, CO, USA, HTTP://OpenMOPAC.net., 2008.
55. http://limor1.nioch.nsc.ru/quant/program/conformers/.
56. C. F. Macrae, I. J. Bruno, J. A. Chisholm, P. R. Edgington, P. McCabe, E. Pidcock, L. Rodriguez-Monge, R. Taylor, J. van de Streek, P. A. Wood, Mercury, *J. Appl. Crystallogr.*, 2008, **41**, 466.
57. C. F. Macrae, P. R. Edgington, P. McCabe, E. Pidcock, G. P. Shields, R. Taylor, M. Towler, J. van de Streek, *J. Appl. Crystallogr.*, 2006, **39**, 457.

Received January 19, 2011;
in revised form April 20, 2011